Modeling the Compressive Stress–Strain Response of Polymeric Foams

G. Spathis, E. Kontou

Department of Applied Mathematical and Physical Sciences, Section of Mechanics, National Technical University of Athens, 5 Heroes of Polytechnion, Athens GR-15773, Greece

Received 28 December 2009; accepted 1 December 2010
DOI 10.1002/app.33848
Published online 11 April 2011 in Wiley Online Library (wileyonlinelibrary.com).

ABSTRACT: The mechanical behavior of cellular materials appears to have, for both open and closed cells, similar characteristics. The compressive stress–strain diagram contains a nearly elastic regime; this leads to a limit load, followed by a plateau extending to a strain of about 50% on average. All of the main features of this curve are related to the material's microstructure. In this study, taking into account the complex deformation mechanisms occurring in a cellular material under external loading, we introduced a statistical micromechanics model. The geometry of our analysis was based on a previous study, where the deformation of the individual struts was connected to the macroscopic deformation tensor. Assuming further that deformation was separated into elastic and viscoplastic parts and following a specific kinematic procedure, we simulated the compressive stress–strain response, the rate dependence, and the loading–unloading behavior of polymeric foam materials. © 2011 Wiley Periodicals, Inc. J Appl Polym Sci 121: 3262–3268, 2011

Key words: compression; mechanical properties; microstructure; modeling

INTRODUCTION

Cellular solids may be distinguished as natural materials, such as wood, cork, cancellous bone, sponge, and coral, or synthetic materials, such as metals, honeycombs, and foams. They can have either open cell faces (open cells) connected with struts or they can be covered by plates or membranes (closed cells). Synthetic cellular materials can be made from all main material types, including metals, polymers, ceramics, paper, and carbon. Foams may appear with a variety of densities, which are a few percentage of the density of the base material.[1] In all these cases, a microstructure consisting of an interconnected network of cells with nearly straight edges is the main characteristic. This specific microstructure is responsible for a variety of properties, such as a high bending stiffness, that have made metal foams a competitive engineering material in recent years.[2] Metallic foams used in sandwich panels between two dense solids lead to an increase in the moment of inertia with a minimum increase in weight. Polymer and metal foams are useful in a large number of very important applications, from daily life packaging of materials to energy collection systems.

Correspondence to: E. Kontou (ekontou@central.ntua.gr).

Journal of Applied Polymer Science, Vol. 121, 3262–3268 (2011)

Basic information on cellular materials, including their microstructure, density, and mechanical properties, was given in a book by Gibbson and Ashby.[3] Apart from this, many publications have dealt with the manufacturing, design, properties, and applications of these materials.[4–6]

With regard to the mechanical behavior of cellular materials, most foams, both open and closed cells, exhibit similar characteristics. In a compressive stress–strain diagram (Fig. 1), there is a nearly linear elastic regime (region I); this leads to a limit load, which is followed by a plateau (region II), which extends to a strain of about 50% on average.[7] Thereafter, a stiffening stress region manifests (region III). The initial region is related to the small bending deformation of the struts of the microstructure. As the compressive strain increases, there is a critical value where a high number of individual struts, which are almost aligned with the loading axis, become unstable, buckle elastically or plastically, and exhibit the plateau region II. Upon higher values of compressive strain, a large number of struts come into contact, and this effect is expressed by the densification region III. At this stage, the material approaches the intrinsic response of a solid-phase material. The load peak is considered to be related to the onset of the instability, which is initially localized, then diffused through the specimen, and requires approximately the same stress value (plateau region).[7] The material response becomes stable again in the densification region.

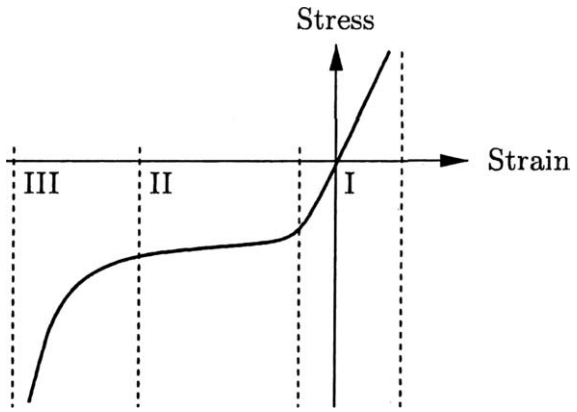

Figure 1 Typical compressive stress–strain response of a cellular solid.

A lot of micromechanical models have been developed[8–10] to describe the main features of the foam's mechanical response. To this trend, it was found that honeycombs exhibit a similar response to foams;[11,12] therefore, it was used as a model material. Moreover, the elastic/hyperelastic behavior of cellular solids was examined in the studies reported in refs. 1,13, and 14.

Given that the effective mechanical behavior of solid foams is controlled by the cell morphology, which links the macroscopic mechanical properties with the mesoscopic structural parameters, a homogenization of the heterogeneous structure of the cellular material is required. To analyze the response of foams, one needs to combine the beam theory with scaling laws, that is, to approximate an average cell by a simple beam model and calculate the material properties in terms of a homogenization procedure.[3] It has been shown that this treatment is adequate for honeycombs and open-cell foams but not for closed-cell ones.[15] The multiphasic nature of these materials has also been described by continuum models based on the theory of porous media.[16,17]

On the other hand, foams based on polymers usually exhibit large viscoelastic or viscoplastic deformations when they are subjected to compression. Each cell undergoes complex deformation mechanisms, which result in a nonlinear stress–strain behavior.[15]

To describe the aforementioned mechanical behavior of foams, special treatment is required for every discrete region. The elastic region and the onset of instability can be found from characteristic cell-type analysis, whereas the plateau region requires a finite size model to be simulated.

Gong et al.[1] emphasized that the modeling of this response requires an analytical and accurate representation of the microstructure geometry and measurements and modeling of the constitutive behavior of the base material. Following these requirements, Gong and coworkers[1,18] developed a series of models predicting the mechanical response of a set of polyester urethane foams with various cell sizes and densities.

To this trend, the large strain response under the complex loading conditions of foams was analyzed by two- and three-dimensional hyperelastic models.[19]

In this study, the compressive stress–strain response of polymeric foams was analyzed in the frame of viscoplasticity with the use of a statistical micromechanics model. This model deals with the distributed orientations of the foam's struts with respect to the loading axis and introduces a relationship between the macroscopic stretch ratio and the stretch ratio of an individual strut. We took into account the fact that after the initial elastic region, the observed stress overshoot denoted the onset of strut buckling and postbuckling, and the total deformation was separated into an elastic and viscoplastic (inelastic) part in terms of a proper kinematic description.[20,21] The proposed model was proven to successfully simulate the compressive stress–strain curves, the rate effect, and the hysteresis loop of polymeric foams, as studied experimentally elsewhere.[1]

MODEL OF STATISTICAL MICROMECHANICS

Hård af Segerstad et al.[7] developed a model of an open-cell flexible cellular solid consisting of a network of struts. As shown in Figure 2, each strut was connected to two vertex points that moved affinely in the large deformation regime, and the strut was characterized by the vertex-to-vertex vectors $\mathbf{r}_{0_i}$ and $\mathbf{r}_i$ in the reference and current configurations, respectively, so that

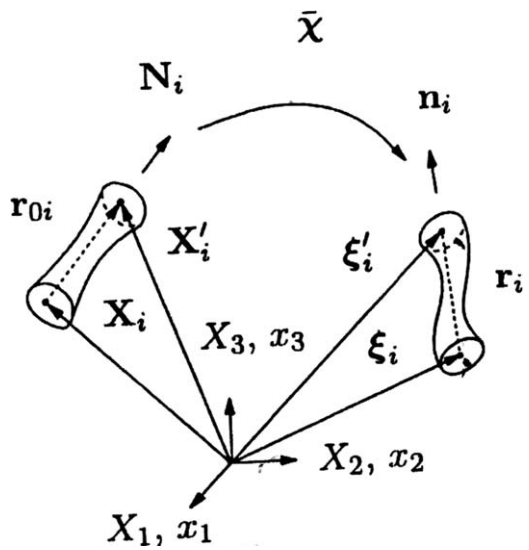

Figure 2 Affine motion of the strut vertices in the large-strain (postbuckling) regime after Hård af Segerstad et al. X_i, X_i', $\xi i'$, $\xi i'$ are the position vectors of strut i at the initial and current configuration. $\bar{X}$ is the macroscopic deformation map.

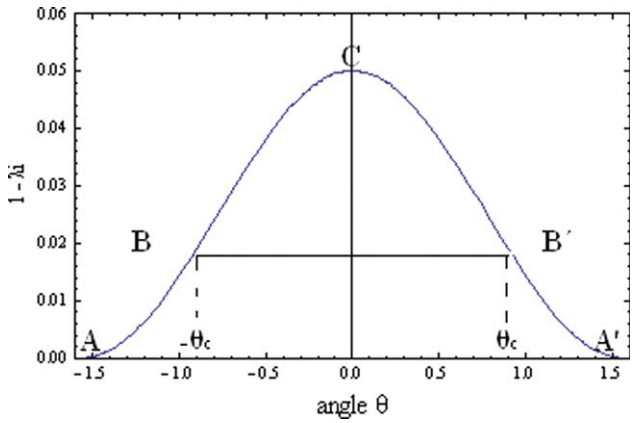

Figure 3 Schematic presentation of λ_i with respect to θ, given by eq. (4). [Color figure can be viewed in the online issue, which is available at wileyonlinelibrary.com.]

$$\mathbf{r_{0_i}} = \mathbf{r_{0_i}} N_i \tag{1}$$

$$\mathbf{r_i} = \mathbf{r_i} n_i \tag{2}$$

where N_i and n_i are the material and spatial directors of the strut, respectively, and $\|N_i\| = \|n_i\| = 1$.

In region II, the strains are higher, and the struts are driven in the postbuckling regime. It is assumed[7] that the vertex motion is approximately affine. Following these assumptions and to define an objective measure of strut deformation, Hård af Segerstad et al. introduced the longitudinal stretch ratio of the i (λ_i) strut as follows:

$$\lambda_i = \|\mathbf{r_i}\|\|\mathbf{r_{0_i}}\|^{-1} = \left(N_i \bar{\mathbf{C}} N_i\right)^{1/2} \tag{3}$$

where $\overline{\mathbf{C}} = \overline{\mathbf{F}}^{\mathbf{T}} \cdot \overline{\mathbf{F}}$ is the macroscopic right Cauchy–Green deformation tensor, $\overline{\mathbf{F}}$ is the deformation gradient tensor, $\overline{\mathbf{F}}^{\mathbf{T}}$ is the transposed tensor.

With the reasonable assumption that there is a two-dimensional problem in the case of isotropic foam, the analytical expression for λ_i, by eq. (3), is given by

$$\lambda_i = \left(\lambda_1^2 \cos^2\theta + \lambda_2^2 \sin^2\theta\right)^{1/2} \tag{4}$$

where θ is the angle between the loading axis and vector $\mathbf{r_0}$ and λ_1 and λ_2 are the macroscopic principal stretch ratios in the longitudinal and lateral directions, respectively.

In our analysis, starting from an individual strut, we assumed that in the undeformed state, all struts are randomly distributed and formed an initially isotropic material. When the compressive load is applied, the elastic bending of the struts is initiated, especially for the group of struts that form low values of θ; this results in the initial elastic slope (region I) of the stress–strain curve. As loading proceeds, even a higher number of struts is subjected to bending, whereas some of them are already in the postbuckling region. When a sufficient population of struts is transferred in the postbuckling stage, it is macroscopically manifested by the onset of region II and is accompanied by the corresponding plateau stress value. Under this unstable situation, no further stress increment for higher strain values is required. This mechanism was analytically formulated in terms of a distribution function, which arose from the analytical expression of λ_i, as expressed by eq. (4). Therefore, the object of our analysis was the way the population of the struts, which constituted the foam material, are distributed in different directions (θ's) in respect to the loading axis. The type of this distribution determines the onset of region II, and consequently, the macroscopic stretch ratio, which manifests this transition.

By plotting eq. (4) with respect to θ, we obtained a normal-type distribution function, as shown in Figure 3, which appeared to have a maximum value around the value zero for θ. From this schematic presentation, it was revealed that when the strut was slightly inclined in respect to the loading axis, it underwent a high value of λ_i, which was driven thereafter to the postbuckling stage. The integration of the area (ACA′) under this function expressed the fraction of struts that had experienced λ_i when the longitudinal macroscopic stretch ratio was equal to λ_1, with the limits of integration varying from $-\pi/2$ to $\pi/2$. On the other hand, there was a critical macroscopic stretch ratio (λ_c), which manifested the onset of buckling and postbuckling thereafter. By solving eq. (4) with respect to this λ_c, we evaluated a pair of values for θ_c, where θ_c, is a critical value of angle θ corresponding to λ_c. The struts that were inclined at values lower than θ_c underwent the transition to the buckling/postbuckling stage. By integrating the area (BCB′; see Fig. 3) limited by those angle values and dividing this quantity by the overall area (ACA′) of the distribution function, we obtained the fraction of the struts that underwent the transition to the buckling stage. By inserting a factor ($\dot{k}$), which was related to the average rate of each individual strut to undergo this transition, we obtained a functional form of the rate of the strut transition:

$$\Gamma = \dot{k}\left(\int_{-\theta_c}^{\theta_c} (\lambda_1^2 \cos^2\theta + \lambda_2^2 \sin^2\theta)^{1/2} d\theta\right) \Bigg/ \left(\int_{-\pi/2}^{\pi/2} (\lambda_1^2 \cos^2\theta + \lambda_2^2 \sin^2\theta)^{1/2} d\theta\right) \tag{5}$$

The factor $\dot{k}$ is specified later.

KINEMATIC DESCRIPTION

According to the aforementioned mechanical response of the foams, it was reasonable to assume that the strain developed in the polymeric foam material could be separated into a viscoplastic (or inelastic) part, which corresponded to the buckling and postbuckling conditions, and an elastic part, which was related to the effective or driven stress. This separation was treated in a way similar to that in plasticity, where the kinematic formulation introduced by Rubin[21] was implemented. The representative volume element under consideration was foam material containing a large number of cells, and its orientation and elastic deformation was defined by a triad of vectors ($\mathbf{m_i}$). The time evolution $\dot{\mathbf{m}}_\mathbf{i}$ of the vectors $\mathbf{m_i}$ was expressed by $\dot{\mathbf{m}}_\mathbf{i} = \mathbf{L_m m_i}$, where $\mathbf{L_m}$ is the elastic velocity gradient tensor, and $\mathbf{L_m} = \mathbf{L} - \mathbf{L_p}$, where $\mathbf{L}$ is the velocity gradient tensor and $\mathbf{L_p}$ is the plastic velocity gradient tensor and is decomposed into a symmetric part ($\mathbf{D_p}$) and an antisymmetric part ($\mathbf{W_p}$) as follows: $\mathbf{L_p} = \mathbf{D_p} + \mathbf{W_p}$. For physically meaningful constitutive equations for $\mathbf{D_p}$ and $\mathbf{W_p}$, the inequality $\mathbf{T}'\cdot\mathbf{D_p} > 0$ had to be satisfied, where $\mathbf{T}'$ is the deviatoric stress tensor. The details of this theory are presented in ref. According to Rubin, in the case of uniaxial stress, the time derivatives ($\dot{\mathbf{a}}$, $\dot{\mathbf{b}}$, $\dot{\mathbf{c}}$) of the principal stretch ratios (a, b, and c) of a material line element for a plastically orthotropic material are given by

$$\frac{\dot{a}}{a} = \frac{\dot{j}_m}{3j_m} + \mathbf{D'_{11}},\ \frac{\dot{b}}{b} = \frac{\dot{j}_m}{3j_m} + \mathbf{D'_{22}},\ \frac{\dot{c}}{c} = \frac{\dot{j}_m}{3j_m} + \mathbf{D'_{33}} \quad (6)$$

where j_m is the elastic dilatation expressed by

$$p = K\left(\frac{1}{j_m} - 1\right) \quad (7)$$

$\dot{j}_m$ is its time derivative, K is the bulk modulus and p is the hydrostatic pressure. In the case of the uniaxial stress (T_{11}), j_m is given by

$$j_m = \frac{3K}{T_{11} - 3K} \quad (8)$$

where $\mathbf{D'_{ij}}$ are the components of the deviatoric symmetric part ($\mathbf{D}$) of the total velocity gradient tensor, which after Rubin are given by the following equations:

$$\mathbf{D'_{11}} = \frac{\dot{a}_m}{a_m} + \frac{\Gamma}{18}\frac{T_{11}}{\mu J_m^{-1}}[4b_{11}a_m^6 + (b_{22} + b_{33})] \quad (9a)$$

$$\mathbf{D'_{22}} = -\frac{1}{2}\frac{\dot{a}_m}{a_m} + \frac{\Gamma}{18}\frac{T_{11}}{\mu J_m^{-1}}[2b_{11}a_m^6 + (2b_{22} - b_{33})] \quad (9b)$$

$$\mathbf{D'_{33}} = -\frac{1}{2}\frac{\dot{a}_m}{a_m} + \frac{\Gamma}{18}\frac{T_{11}}{\mu J_m^{-1}}[2b_{11}a_m^6 + (-b_{22} + 2b_{33})] \quad (9c)$$

where μ is the shear modulus, α_m is the elastic stretch ratio, $\dot{\mathbf{a}}_\mathbf{m}$ its time derivative, Γ is a nonnegative function that needs to be specified, and b_{ij} are nonnegative constants, which in the case of elastically isotropic material are taken as equal to unity.

When eqs. (6), (8), and (9a) are combined, the rate evolution of α_m is of the form:

$$\frac{\dot{a}_m}{a_m} = \frac{\dot{a}}{a} + \frac{\dot{a}_m 2\mu(1+\nu)}{3[a_m 2\mu(1+\nu) - 3K]} - \frac{\Gamma}{12}\left(\frac{T_{11}}{\mu J_m^{-1}}\right)(4b_{11}a_m^6 + b_{22} + b_{33}) \quad (10)$$

where α is the longitudinal stretch ratio, ν is the Poisson ratio, and $\dot{\alpha}$ is the imposed strain rate. The quantity Γ is considered to define the rate of transition in the buckling state. When the plateau region is initiated, the effect that is subsequent to the stress peak ($\dot{\alpha}_m$) is taken to be zero, and α_m is equal to λ_c, where λ_c is the critical stretch ratio relative to the onset of postbuckling. With this specific condition applied to eq. (10), and after some obvious approximations, because of the fact that α_m is close to unity, eq. (10) leads to an expression of a critical rate (Γ_c) as follows:

$$\Gamma_c = \frac{\dot{\alpha}}{\alpha(\lambda_c - 1)} \quad \text{or} \quad \Gamma_c = \frac{\dot{\alpha}}{\lambda_1(\lambda_c - 1)} \quad (11)$$

where α has been replaced with the symbol λ_1 for reasons of uniformity.

Considering that at this critical point, $\Gamma = \Gamma_c$, the value of factor $\dot{k}$ of eq. (5) can be calculated and because the distribution function is symmetric, we have

$$\dot{k} = \Gamma_c \quad (12)$$

Combining eqs. (5), (11), and (12), we obtain

$$\Gamma = \frac{\dot{\alpha}}{\lambda_1(\lambda_c - 1)}\left(\int_{-\theta_c}^{\theta_c} (\lambda_1^2\cos^2\theta + \lambda_2^2\sin^2\theta)^{1/2}d\theta\right) \Bigg/ \left(\int_{-\pi/2}^{\pi/2} (\lambda_1^2\cos^2\theta + \lambda_2^2\sin^2\theta)^{1/2}d\theta\right) \quad (13)$$

Equation (13) expresses the rate of strut transition to the buckling stage, where $\dot{\alpha}$ is the imposed strain rate and λ_1 and λ_2 are the macroscopic longitudinal and transverse stretch ratios, respectively.

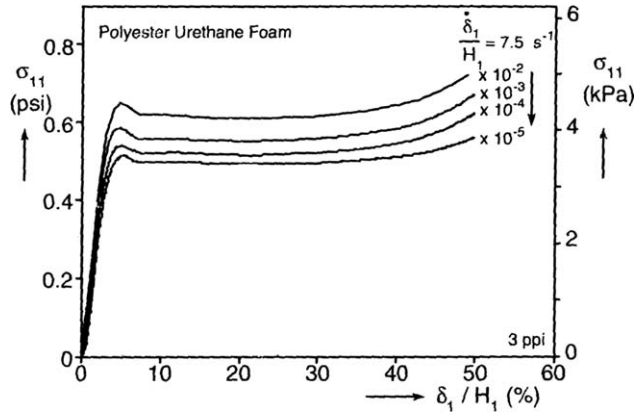

Figure 4 Compressive stress–strain data of a poly(ester urethane) foam (3 ppi) at various strain rates $\dot{\delta}_i/H_1$ after Gong et al.[1]

APPLICATION OF THE PROPOSED MODEL TO THE COMPRESSIVE BEHAVIOR OF POLYMERIC FOAMS

Compressive stress–strain behavior

The proposed analysis was validated by a simulation of the experimental results of the study by Gong et al.[1] The foams analyzed in their study were based on ester resin, diisocyanate, water, catalysts, and surfactants, and the geometric and material parameters are discussed in detail in ref. [1]. Compressive tests were performed, and it was found that the mechanical properties of the foam polymers studied depended on the rate of loading, which meant that they exhibited a viscoelastic response. In Figure 4, the representative experimental results of the rise direction response from the study by Gong et al. are presented for a foam of a specific nominal cell size [3 pores per inch (ppi)] at four distinct displacement rates $\dot{\delta}_i/H_1$, which varied from 7.5×10^{-2} to 7.5×10^{-5} s^{-1}. With increasing strain rate, the initial modulus stiffened, the maximum stress increased, too, and the whole curve moved to higher values of stress level.

To simulate the experimental data, apart from the elastic constants values, that is, μ and ν, the experimental strain rate $\dot{\alpha}$ and λ_c were incorporated into eqs. (10) and (13). ν was taken to be equal to 0.5 for the strain range examined, according to the experimental data of Widdle et al.[22] α_m could then be evaluated at every stage of deformation through integration of eq. (10). The integration of eq. (10) was made numerically with small time steps with the software Mathematica[23] until a high convergence was achieved.

From the performed integrations, we found that the variation of α_m with respect to the total strain was of the form of the compressive stress–strain curve. Therefore, by simply multiplying it by the Young's modulus of the material (taken from the initial slope of the stress–strain curve), we obtained the simulated compressive stress–strain curve.

More specifically, the experimental results were simulated as follows: the stress–strain curve of the lower strain rate of 7.5×10^{-5} s^{-1} was modeled by the aforementioned procedure. The model parameters required were the initial slope of the stress–strain curve, which was the foam material's modulus (E) equal to 125 kPa and λ_c, given by the experimental data, equal to 0.954. To obtain the part of the densification region III, which is presented in the experimental results, an ideal elastomer's constitutive equation was applied. This was a reasonable assumption because at this stage of deformation, the elastomeric features of the foam material were manifested. Therefore, the response at this region was simulated with an extra stress term (σ_h), which was given by[24]

$$\sigma_h = C_r\left(\lambda_1 - \frac{1}{(\lambda_1)^2}\right) \tag{14}$$

where C_r is a hardening modulus equal to 0.5 kPa. To obtain the stress–strain data for all of the strain rates examined, a scaling rule, valid in viscoelasticity, was applied. According to this rule, proposed by Matsuoka,[25] a stress–strain curve obtained at the rate $\dot{r}_1$ could be predicted from an experimental stress–strain curve at a rate $\dot{r}$ by the multiplication of the stress and strain values by the scaling factor $[(\dot{r}_1/\dot{r})^n]$ and $[(\dot{r}_1/\dot{r})^m]$ for the stress and strain, respectively. In this way, all of the stress–strain curves for the four strain rates were simulated, with respect to that at 7.5×10^{-5} s^{-1}. The parameters m and n were fitted to be equal to 0.04. The simulated compressive stress–strain results are shown in

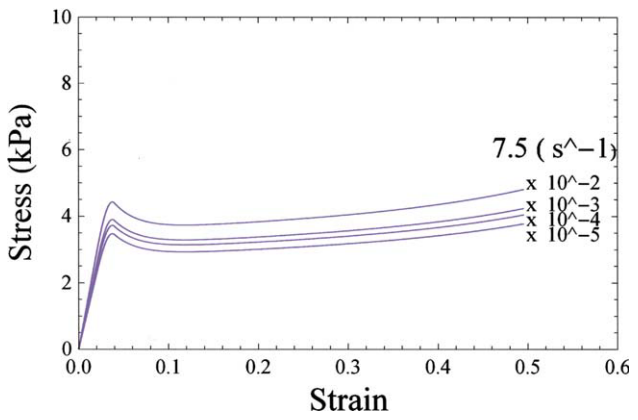

Figure 5 Model simulations of the experimental results of Figure 4. [Color figure can be viewed in the online issue, which is available at wileyonlinelibrary.com.]

Figure 5, and a very good agreement with the experimental data shown in Figure 4 was obtained.

Compressive loading–unloading behavior

In the study by Gong et al.,[1] the loading–unloading response of the foam materials was studied and is presented in Figure 6. The stress–strain data of the first cycle are shown in this figure; they exhibited a nonlinear unloading curve, with a small value of residual strain. The stress during unloading was simply the reversed stress–strain behavior of the foam material, which was a tensile mode of deformation, which started from the densified stage, where the foam material was depressed approximately at a strain of 50%. The calculation of this stress was performed as discussed in the first paragraph of this section and with a now lower value of Young's modulus (because of the different behavior of the densified material), which was fitted equal to 12 KPa. To simulate the unloading behavior, we also took into account the fact that all of the struts were in the buckling (or postbuckling) condition. Therefore, the distribution density function had to be modified accordingly. λ_c was now defined as the position where the majority of struts were recovering, and this effect took place at a value approximately equal to $1 - \lambda_c$.

The model simulations of the experimental data of Figure 6 are presented in Figure 7 and exhibited a satisfactory agreement between the experiment and the model simulations.

CONCLUSIONS

In this study, a statistical micromechanics model for describing the compressive stress–strain response of the cellular materials was examined. The model was based on the expression of the stretch ratio of an individual strut with respect to the macroscopic longitudinal stretch ratio and the angle between the loading axis and the axis of the strut itself. After some reasonable assumptions, this expression was transformed to a probability density function with respect to the macroscopic strain. Hence, a functional form of the rate of strut transition from the elastic region to the buckling stage was defined. This rate will be treated hereafter as the rate of inelastic strain formation in a way similar to plasticity or inelasticity. Applying a specific kinematic formulation, we achieved the constitutive description of the foam material.

The proposed analysis was proven to successfully describe the compressive stress–strain response of the polymeric foams, the exhibited rate dependence, and the loading–unloading stress–strain response.

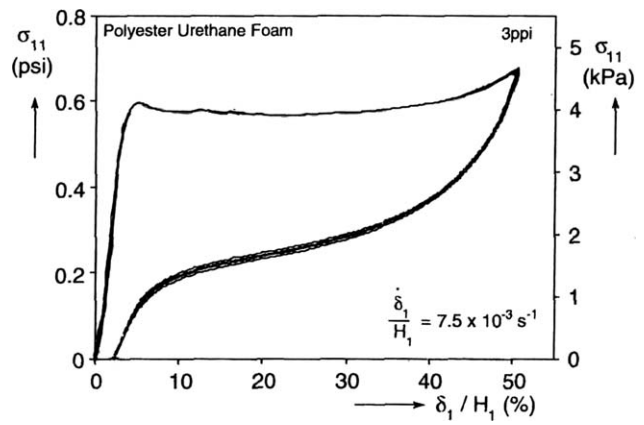

Figure 6 Compressive loading–unloading stress–strain response of a poly(ester urethane) foam (3 ppi) after Gong et al.[1]

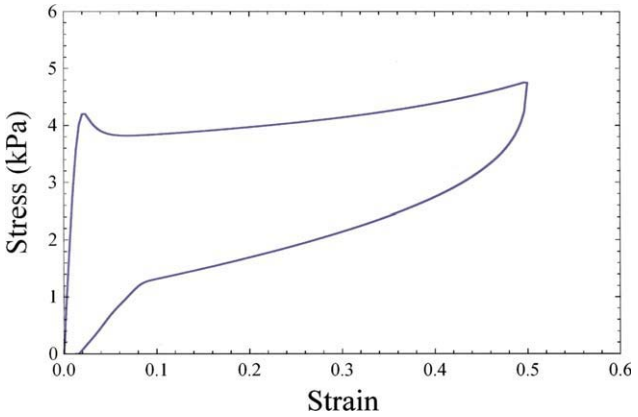

Figure 7 Model simulations of the experimental data of Figure 6. [Color figure can be viewed in the online issue, which is available at wileyonlinelibrary.com.]

References

1. Gong, L.; Kyriakides, S.; Jang, W.-Y. Int J Solid Struct 2005, 42, 1355.
2. Tekoglu, C.; Onck, P. R. J Mater Sci 2005, 40, 5911.
3. Gibson, L. J.; Ashby, M. F. Cellular Solids: Structure and Properties, 2nd ed.; Cambridge University Press: Cambridge, England, 1997.
4. Weaire, D.; Hutzler, S. The Physics of Foams; Oxford University Press: Oxford, 1999.
5. Gibbson, L. J. Cell Solids MRS Bull 2003, 28(4), 270.
6. Ashby, M. F.; Evans, A.; Fleck, N. A.; Gibson, L. J.; Hutchinson, J. W.; Wadley, H. N. G. Metal Foams: A Design Guide; Butterworth-Heinemann: Woburn, MA, 2000.
7. Hård af Segerstad, P.; Larsson, R.; Toll, S. Int J Plast 2008, 24, 896.
8. Gent, A. N.; Thomas, A. G. Rubber Chem Technol 1963, 36, 597.
9. Gibson, L. J.; Ashby, M. F.; Schajer, G. S.; Robertson, C. I. Proc R Soc London Sect A 1982, 382, 25.
10. Choi, J. B.; Lakes, R. S. Int J Mech Sci 1995, 37, 51.
11. Zhu, H. X.; Knott, J. F.; Mills, N. J. J Mech Phys Solids 1997, 45, 319.

12. Patel, M. R.; Finnie, I. J Mater 1970, 5, 909.
13. Li, K.; Gao, X.-L.; Roy, A. K. Compos Sci Tech 2003, 63, 1769.
14. Li, K.; Gao, X.-L.; Roy, A. K. Compos B 2004, 36, 249.
15. Ehlers, W.; Markert, B. Int J Plast 2003, 19, 961.
16. Bowen, R. Int J Eng Sci 1982, 20, 697.
17. Larsson, J.; Larsson, R. Comp Methods Appl Mech Eng 2002, 191, 3885.
18. Gong, L.; Kyriakides, S. Int J Solids Struct 2005, 42, 1381.
19. Deminary, S.; Becker, W.; Hohe, J. Mech Mater 2006, 38, 985.
20. Spathis, G.; Kontou, E. J Appl Polym Sci 2001, 79, 2534.
21. Rubin, M. B. Int J Solids Struct 1994, 31, 2653.
22. Widdle, R. D., Jr.; Bajaj, A. K.; Davies, P. Int J Eng Sci 2008, 46, 31.
23. Wolfram, S. Mathematica: A System for Doing Mathematics by Computer, 4th ed.; Addison-Wesley: New York, 1999.
24. Treloar, L. R. G. The Physics of Rubber Elasticity, 3rd ed.; Clarendon: Oxford, 1975.
25. Matsuoka, S. Relaxation Phenomena in Polymers, 2nd ed.; Hanser: New York, 1992; Chapter 3.